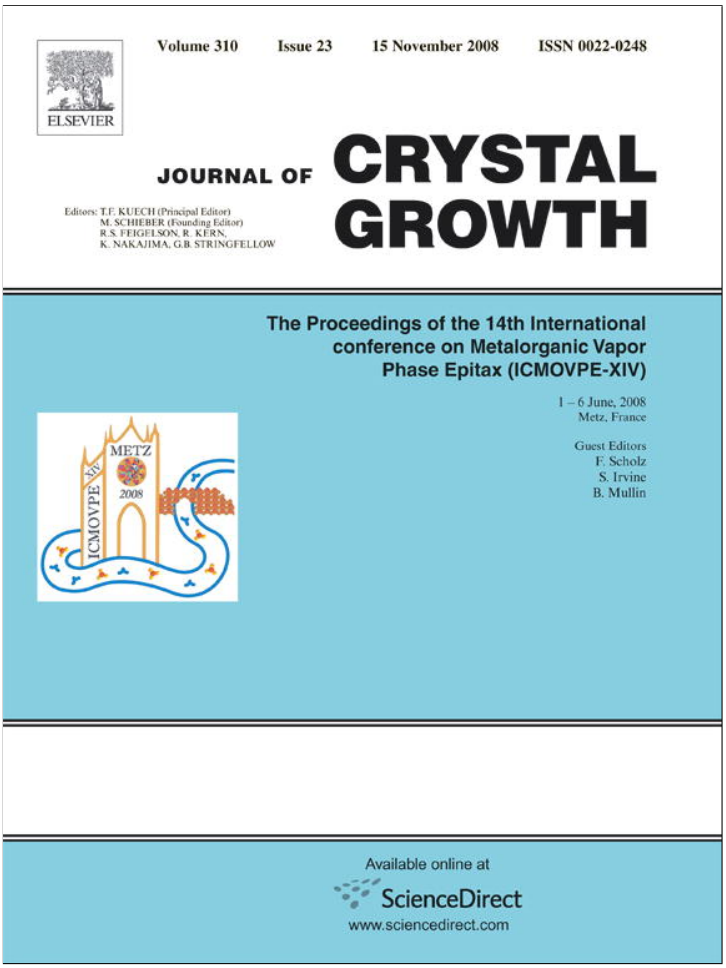

Journal of Crystal Growth 310 (2008) 4867–4870

Contents lists available at ScienceDirect

Journal of Crystal Growth

journal homepage: www.elsevier.com/locate/jcrysgro

Process optimization for the effective reduction of threading dislocations in MOVPE grown GaN using in situ deposited SiN_x masks

J. Hertkorn [a,*], F. Lipski [a], P. Brückner [a], T. Wunderer [a], S.B. Thapa [a], F. Scholz [a], A. Chuvilin [b], U. Kaiser [b], M. Beer [c], J. Zweck [c]

[a] Institut für Optoelektronik, Universität Ulm, Albert-Einstein-Allee 45, D-89081 Ulm, Germany
[b] Materialwissenschaftliche Elektronenmikroskopie, Universität Ulm, Albert-Einstein-Allee 11, D-89081 Ulm, Germany
[c] Institut für Experimentelle und Angewandte Physik, Universität Regensburg, Universitätsstr. 31, D-93051 Regensburg, Germany

ARTICLE INFO

Available online 30 July 2008

PACS:
81.05.Ea
81.15.Gh
78.55.−m
61.10.Nz
79.60.Jv

Keywords:
A1. Atomic force microscopy
A1. High resolution X-ray diffraction
A1. Nucleation
A3. Metalorganic vapor phase epitaxy
A3. Selective epitaxy
B1. Nitrides

ABSTRACT

In this study the in situ deposition of SiN_x masks by metalorganic vapor phase epitaxy (MOVPE) has been optimized to achieve *c*-plane oriented GaN layers on sapphire with a dislocation density $<2\times10^8\,cm^{-2}$. The defect termination was found to be most efficient if the SiN_x is located after the growth of 100 nm GaN, whereas deposited directly on the AlN nucleation it was less efficient but yielded highly compressively strained layers indicated by a donor bound exciton peak position of 3.493 eV in photoluminescence (13 K). Furthermore we observed by in situ reflectometry that a higher deposition temperature during the silane treatment was strongly increasing the surface roughening yielding a faster coalescence during the GaN overgrowth but finally influencing the defect termination negatively. In terms of lateral overgrowth a high V/III ratio (2D growth mode) was most efficient in terms of defect reduction, whereas a 3D–2D-process at lower V/III ratio yielded much faster overgrowth but influenced the defect termination negatively.

1. Introduction

Group III-nitrides as key materials for light-emitting diodes (LEDs) and laser diodes (LDs) still have to be grown on foreign substrates, as GaN wafers are still rare and expensive. Using *c*-plane oriented sapphire (Al_2O_3), the large lattice mismatch between the GaN epitaxial layer and the applied substrate typically yields high dislocation densities up to $3\times10^9\,cm^{-2}$. Such crystal imperfections are known to affect the electrical and optical properties of GaN-based devices negatively, as they act as centers of nonradiative carrier recombination [1–3] and lead to degradation of LDs [4]. The in situ deposition of SiN_x, acting as a nano-mask and influencing the morphology of the overgrown GaN layer, was found to be a fast and simple method leading to a defect reduction [5–15].

In order to get a better understanding of this procedure, we investigated the influence of the SiN_x mask position, the SiN_x deposition temperature and time, as well as the influence of the regrowth conditions used during the lateral overgrowth of the SiN_x mask.

2. Experimental procedure

The samples were grown by metalorganic vapor phase epitaxy (MOVPE) in an AIXTRON 200/RF-S horizontal flow reactor. The process temperature was controlled with a fiber coupled pyrometer faced to the backside of our rotation tray. All the growth temperatures mentioned below are not the real substrate temperatures but the read-out of this pyrometer. Thus the temperature values we provide are expected to be higher than the substrate temperature.

The layers were deposited on 2 in *c*-plane (0 0 0 1) epi-ready sapphire wafers using an oxygen doped AlN nucleation layer (NL) [16]. Further details about the NL deposition and the subsequent GaN growth are given elsewhere [17]. As precursors we used trimethyl-aluminum (TMAl), trimethyl-gallium (TMGa) and high purity ammonia (NH_3). Pd-diffused hydrogen was used as carrier gas.

The SiN_x was deposited either directly on the NL or after the growth of an undoped GaN buffer of variable thickness, using a NH_3 flow of 500 sccm, a reduced reactor pressure of 100 mbar and a SiH_4 molar flow of 0.1 μmol/min. The nano-mask finally was overgrown by undoped GaN yielding an overall layer thickness of 2−3 μm. The crystal quality of our layers was evaluated by low

* Corresponding author. Tel.: +49 731 50 26195; fax: +49 731 50 26049.
E-mail address: joachim.hertkorn@uni-ulm.de (J. Hertkorn).

0022-0248/$ - see front matter © 2008 Elsevier B.V. All rights reserved.
doi:10.1016/j.jcrysgro.2008.07.075

temperature (13 K) photoluminescence (PL) and high resolution X-ray diffraction (HRXRD). The X-ray FWHM values are determined without using any slits on the detector side. The dislocation density of our layers was determined by atomic force microscopy (AFM) after an HCl etch in our hydride vapor phase epitaxy (HVPE) system [18–20]. Transmission electron microscopy (TEM) was used to get information about the SiN_x nano-mask and the dislocation propagation, respectively. The surface properties on a μm and nm scale were investigated by scanning electron microscopy (SEM) or AFM, respectively. To estimate the SiN_x coverage indirectly, the growth process was stopped after the SiN_x deposition and a short GaN overgrowth of about 1 min. Using AFM the areas where the growth of GaN was possible could be determined and thus the relative SiN_x coverage between samples could be calculated.

3. Influence of SiN deposition temperature

In our first growth experiments we deposited 3 min $SiN_x(t_{SiN})$ subsequent to the growth of a 350 nm thick undoped GaN buffer. Hereby the SiN_x deposition temperature T_{SiN} was varied in the range of 1060–1090 °C. The SiN_x mask finally was overgrown with undoped GaN using a two step process (2D-process, Table 1). Hereby lateral growth (2D) was initialized during the first 5 min while the TMGa flow was ramped up continuously to 82 μmol/min finally yielding a GaN growth rate of 2.4 μm/h. For the second step (standard GaN) the growth conditions remained stable for 45 min yielding a GaN surface without any pits.

In agreement with Pakula et al. [11] we could observe by in situ reflectometry that the GaN surface is roughened during the SiN_x deposition. The roughening was found to be stronger with higher T_{SiN}. Therefore, we stopped the process in some additional experiments immediately after the SiN_x masking. Hereby we could observe that the SiH_4 treatment caused the formation of GaN nano-islands (Fig. 1). A high rms surface roughness of 4 nm on a 1 μm^2 scan area was determined by AFM. R_{max} was found to be 36 nm. The average size of such nano-islands was found to be smaller with higher T_{SiN}. In high resolution TEM we finally observed that the SiN_x mask was located in different heights, as indicated by the arrows in Fig. 2. Thus we concluded that the surface roughening and the SiN_x growth are in competition, finally influencing the defect termination (Fig. 3). Based on the data from HRXRD and EPD counting, a SiN_x deposition temperature of 1070 °C was found to be ideal.

Additionally we observed by in situ reflectometry that the lateral overgrowth of the SiN_x mask was slowed down with the reduction of T_{SiN}. In additional experiments we therefore investigated the SiN_x coverage of the different samples. Unexpectedly it could be estimated to be in the range of 55% independent of the SiN_x deposition temperature. In further experiments we therefore deposited two times SiN_x (3 min) in one growth run at 1060 °C (Exp. 1) or 1090 °C (Exp. 2). Subsequent to each SiN_x deposition GaN was grown for several minutes.

The surface investigated by SEM is shown in Fig. 4. As expected, the typical formation of the GaN microislands took place. Analyzing the layer thickness and taking into account that

Table 1
GaN regrowth conditions after SiN deposition

	2D-process	3D–2D-process		Standard
	2D	3D	2D	GaN
Temp. (°C)	1090	1000	1130	1090
Pressure (mbar)	100	200	100	100
NH_3 (sccm)	2000	500	2000	2000
TMGa (sccm)	5–21	21	10	21
V/III-ratio	4600–1095	290	2200	1095
Duration (min)	5	1	20	Variable

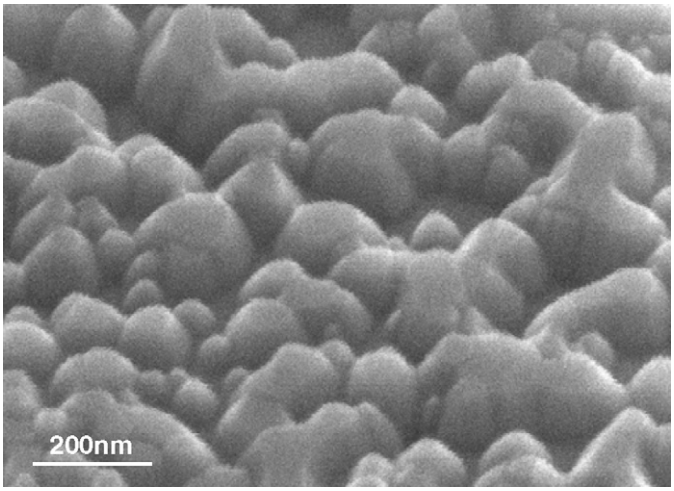

Fig. 1. SEM image of the surface just after the SiN_x deposition. The surface roughening results in the formation of GaN nano-islands.

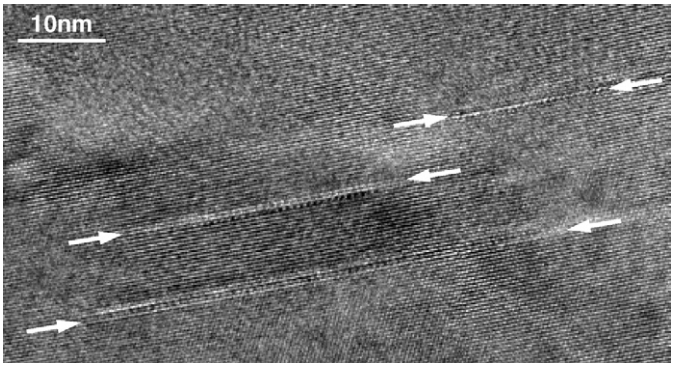

Fig. 2. As a consequence of the surface roughening during the SiN_x deposition, the SiN_x atoms (indicated by arrows) are positioned in different height (HRTEM-picture).

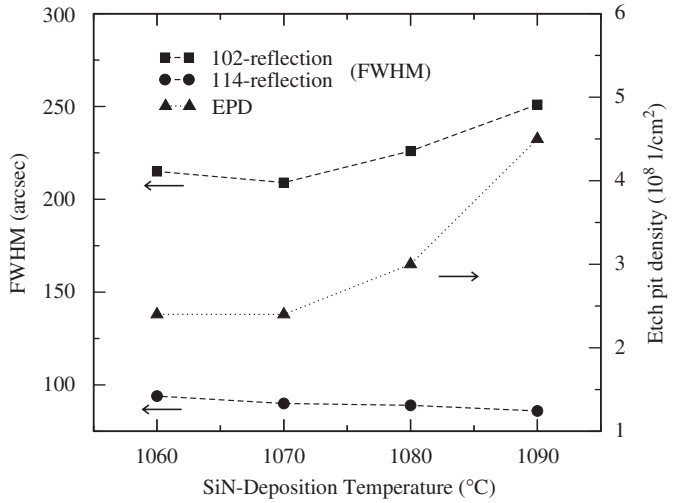

Fig. 3. Influence of T_{SiN} on the GaN quality. The SiN_x was deposited for 3 min after the growth of 350 nm GaN.

SiN_x acts as anti-surfactant, one can conclude that Levels 1 and 2 are indicating the SiN_x positions. The smooth, top most GaN surface is indicated by Level 3.

If the SiN_x was deposited at 1060 °C the Level 1 area is comparably large, indicating the deposition of a stable SiN_x mask yielding high selectivity. If the observed surface roughening during the SiH_4 treatment is too strong (Fig. 4, Levels 1 and 2, $T_{SiN} = 1090$ °C), only low selectivity is observed, finally explaining the faster coalescence yielding worse crystal quality.

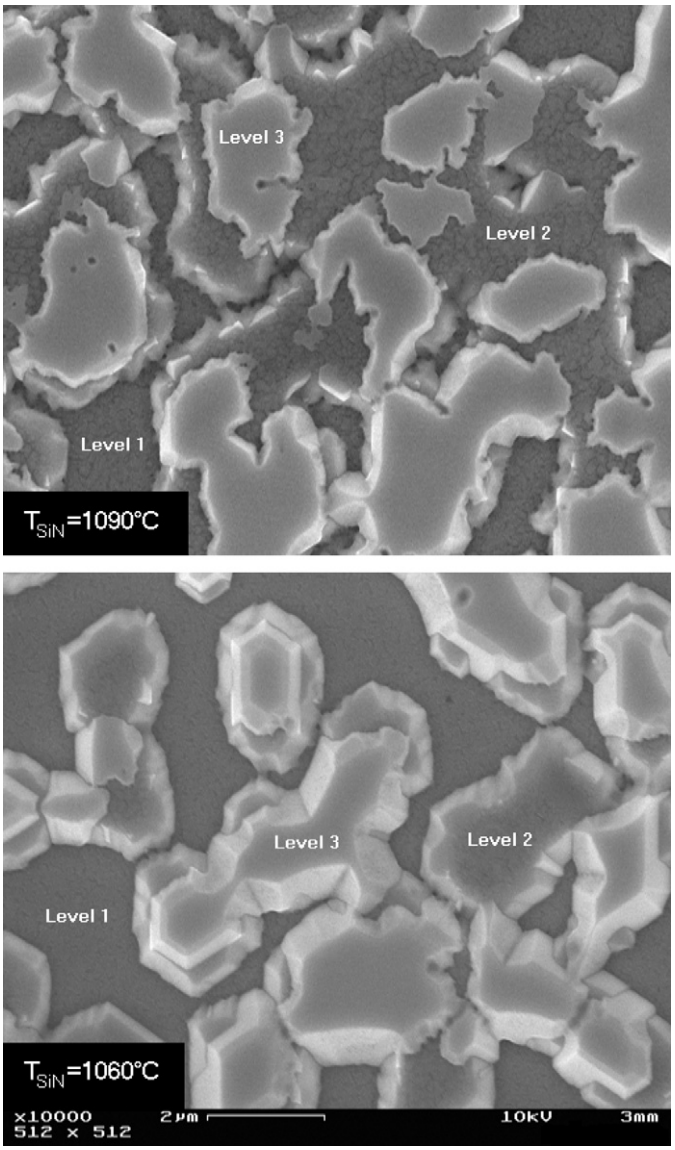

Fig. 4. Influence of T_{SiN} on the selectivity of the SiN_x mask.

4. Influence of growth conditions during lateral overgrowth

Next we investigated the influence of the GaN growth conditions subsequent to the SiN_x masking. The SiN_x was deposited for 3 min at a temperature of 1070 °C after the growth of a 350 nm thick undoped GaN buffer. The regrowth conditions were changed in terms of getting first a 3D growth followed by a second process step where 2D-growth is implemented (3D–2D-process, Table 1). The 3D–2D-growth method is well known from the facet assisted epitaxial lateral overgrowth (FACELO) [21,22].

As expected the 3D growth strongly enforced the GaN microislands formation, as indicated by in situ reflectometry (400 nm signal). Surprisingly the coalescence of such islands happened almost instantaneously during the first minute of the 2D growth. We explain this behavior by the desorption of the thin and fragile SiN_x mask, if the regrowth temperature is exceeding a certain value above T_{SiN}. Hence the resulting quality of the GaN realized with this 3D–2D-process could not compete with the results found in Section 3 (2D-process). Only with a drastically increased SiN_x deposition time ($t_{SiN} = 7$ min) a comparable dislocation reduction could be achieved. Hereby it must be noted that the formation of additional stacking faults caused strongly broadened peaks in HRXRD and PL. Hence we concluded that nonideal regrowth conditions can strongly decrease the ability of the SiN_x to achieve high quality GaN layers.

5. Influence of the SiN position

In our next experiments we investigated the influence of the SiN_x position on the GaN quality. For these we chose $T_{SiN} = 1070$ °C, $t_{SiN} = 4$ min and the regrowth was done with the 2D-process introduced in Section 3. The SiN_x was deposited either directly on the AlN NL or after the growth of 15, 50, 100, 350 and 1000 nm of undoped GaN, respectively.

By EPD measurements we observed that the dislocation reduction took place almost independent of the SiN_x position (Table 2) and yielded values down to 1.6×10^8 cm^{-2}.

PL measurements pointed out that the layers are heavily compressively strained. From the position of the donor-bound exciton (D^0X) line we deduce a maximum compressive biaxial strain of up to $\varepsilon_\perp = 1.4 \times 10^{-3}$ with material parameters taken from Ref. [23].

However, the high strain in samples with the SiN_x deposited close to the NL causes the formation of stacking faults (visible in

Table 2
Influence of the SiN position on the etch pit density (EPD), HRXRD and PL (13 K)

SiN position (nm)	PL D^0X-exciton		HRXRD		EPD (1/cm^2)
	Energy (eV)	FWHM (meV)	102-refl. (arcsec)	002-refl. (arcsec)	
0	3.493	2.9	345	385	2.4×10^8
15	3.490	2.0	229	239	1.6×10^8
50	3.485	1.2	234	64	3.4×10^8
100	3.485	1.3	213	81	2.0×10^8
350	3.484	1.2	247	75	1.7×10^8
1000	3.483	1.5	281	73	4.0×10^8

The standard deviation of the EPD is about ±20%.

TEM) also explaining the broadened D^0X linewidth and X-ray peaks, respectively (Table 2). To overcome such problems we deposited a second SiN_x mask after 1.5 μm yielding a PL D^0X-linewidth of 1.4 meV (at 3.491 eV) and drastically narrowed X-ray values.

A lowest FWHM of 1.2 meV for the D^0X-peak was found with SiN_x positioned after the growth of 50, 100 or 350 nm GaN. In HRXRD the 102-refl. shows a minimum for the SiN_x positioned after 100 nm (Table 2). Notice that by measuring our X-ray data with an open detector geometry, it is evident that other broadening mechanisms will add to our FWHM values, in particular strain induced bowing of our samples. As the strain values of all samples are fairly similar, we assume that this does not influence our qualitative interpretation of the results. Additionally, the volume fraction of GaN with high TD density below the SiN_x to that of GaN of lower TD density above the SiN_x does change with the interlayer position. Especially for the samples with the SiN_x positioned after 350 and 1000 nm, this must be taken into account.

6. Conclusion

The growth of high quality GaN buffer layers with a low dislocation density of $<2.0\times10^8\,cm^{-2}$ on sapphire could be achieved by the optimized in situ deposition of SiN_x masks. The best buffer layer was grown with a SiN_x deposition temperature of 1070 °C and a 2D-regrowth process. The ideal position of the SiN_x mask was found to be after the growth of 100 nm undoped GaN.

Acknowledgment

This research was financially supported by Osram Opto Semiconductors and the Bundesministerium für Bildung und Forschung (BMBF). The sample characterization by H. Xu, K. Forghani and H. Kaim is gratefully acknowledged.

References

[1] T. Sugahara, H. Sato, M. Hao, Y. Naoi, S. Kurai, S. Tottori, K. Yamashita, K. Nishino, L.T. Romano, S. Sakai, Jpn. J. Appl. Phys. 37 (1998) L398.
[2] S. Dassonville, A. Amokrane, B. Sieber, J.-L. Farvacque, B. Beaumont, V. Bousqet, P. Gibart, K. Leifer, J.-D. Ganiere, Physica B 273–274 (1999) 148.
[3] S. Dassonville, A. Amokrane, B. Sieber, J.-L. Farvacque, B. Beaumont, P. Gibart, J. Appl. Phys. 89 (2001) 3736.
[4] C.S. Tomiya, H. Nakajima, K. Funato, T. Miyajima, K. Kobayashi, T. Hino, S. Kijima, T. Assano, M. Ikeda, Phys. Status Solidi (a) 188 (2001) 69.
[5] P. Vennéguès, B. Beaumont, S. Haffouz, M. Vaille, P. Gibart, J. Crystal Growth 187 (1998) 167.
[6] S. Sakai, T. Wang, Y. Morishima, Y. Naoi, J. Crystal Growth 221 (2000) 334.
[7] S. Tanaka, M. Takeuchi, Y. Aoyagi, Jpn. J. Appl. Phys. 39 (2000) L831.
[8] O. Contreras, F.A. Ponce, J. Christen, A. Dadgar, A. Krost, Appl. Phys. Lett. 81 (2002) 4712.
[9] X.L. Fang, Y.Q. Wang, H. Meidia, S. Mahajan, Appl. Phys. Lett. 84 (2004) 484.
[10] K.J. Lee, E.H. Shin, K.Y. Lim, Appl. Phys. Lett. 85 (2004) 1502.
[11] K. Pakula, R. Bozek, J.M. Baranowski, J. Jasinski, Z. Liliental-Weber, J. Crystal Growth 267 (2004) 1.
[12] K. Engl, M. Beer, N. Gmeinwieser, U.T. Schwarz, J. Zweck, W. Wegscheider, S. Miller, A. Miler, H.-J. Lugauer, G. Brüderl, A. Lell, V. Härle, J. Crystal Growth 289 (2006) 6.
[13] M.J. Kappers, R. Datta, R.A. Oliver, F.D.G. Rayment, M.E. Vickers, C.J. Humphreys, J. Crystal Growth 300 (2007) 70.
[14] J. Xie, S.A. Chevtchenko, Ü. Özgür, H. Morkoc, Appl. Phys. Lett. 90 (2007) 262112.
[15] A. Bchetnia, A. Touré, T.A. Lafford, Z. Benzarti, I. Halidou, M.M. Habchi, B. El Jani, J. Crystal Growth 308 (2007) 283.
[16] B. Kuhn, F. Scholz, Phys. Status Solidi (a) 188 (2001) 629.
[17] J. Hertkorn, P. Brückner, S.B. Thapa, T. Wunderer, F. Scholz, M. Feneberg, K. Thonke, R. Sauer, M. Beer, J. Zweck, J. Crystal Growth 308 (2007) 30.
[18] T. Hino, S. Tomiya, T. Miyajima, K. Yanashima, S. Hashimoto, M. Ikeda, Appl. Phys. Lett. 76 (2000) 3421.
[19] T. Miyajima, T. Hino, S. Tomiya, K. Yanashima, H. Nakajima, T. Araki, Y. Nanishi, A. Satake, Y. Masumoto, K. Akimoto, T. Kobayashi, M. Ikeda, Phys. Status Solidi (b) 228 (2001) 395.
[20] F. Habel, M. Seyboth, Phys. Status Solidi (c) 0 (2003) 2448.
[21] K. Hiramatsu, K. Nishiyama, M. Onishi, H. Mitzutani, M. Narukawa, A. Motogaito, H. Miyake, Y. Iyechika, T. Maeda, J. Crystal Growth 221 (2000) 316.
[22] F. Habel, P. Brückner, F. Scholz, J. Crystal Growth 272 (2004) 515.
[23] J.-M. Wagner, F. Bechstedt, Phys. Rev. B 66 (2002) 115202.